LETTER

NJC
www.rsc.org/njc

Hybrid non-silica mesoporous thin films

Paula C. Angelomé,[a] Sara Aldabe-Bilmes,[b] Mauricio E. Calvo,[b] Eduardo L. Crepaldi,[c] David Grosso,[c] Clément Sanchez*[c] and Galo J. A. A. Soler-Illia*[ac]

[a] *Unidad de Actividad Química, Comisión Nacional de Energía Atómica, Centro Atómico Constituyentes, Av. Gral Paz 1499, San Martín, B1650KNA Buenos Aires, Argentina. E-mail: gsoler@cnea.gov.ar; Fax: +54 11 6772-7886; Tel: +54 11 6772-7032*

[b] *INQUIMAE-DQIAQF, Facultad de Ciencias Exactas y Naturales, Universidad de Buenos Aires, Ciudad Universitaria Pab. II, C1428EHA Buenos Aires, Argentina*

[c] *Laboratoire de Chimie de la Matière Condensée (CNRS UMR 7574), Université Pierre et Marie Curie, 4 Place Jussieu, 75252 Paris cedex 05, France. E-mail: clems@ccr.jussieu.fr*

Received (in Montpellier, France) 1st October 2004, Accepted 3rd November 2004
First published as an Advance Article on the web 6th December 2004

Large-pore TiO_2 and ZrO_2 mesoporous films with 2D-Hex or cubic mesostructures were prepared by dip-coating. Organic bifunctional molecules presenting an organic function and a complexing grafting group (phosphate, carboxylate) were explored as surface modifiers. The incorporation of these functions into the mesoporous network was monitored by crossed FT-IR and EDS techniques. Leaching experiments in different conditions were performed to assess the anchoring of the grafted groups. While phosphate or phosphonate groups are strongly grafted, carboxylate functions can be released in a pH-dependent way.

Mesoporous hybrid inorganic-organic materials presenting very high surface areas, controlled pore size and tailored organic functions dangling from the walls or embedded into the framework are very promising as multifunctional materials.[1–4] Some targeted applications such as sensors, analytical devices (separation or chromatography), and advanced optoelectronics require thin film processing. In these fields, mesoporous hybrid thin films (MHTF) appear as customised materials that integrate organic functions within tailored pores in a well-defined thin transparent matrix, where short migration distances and large pores favour molecule migration; low thickness and transparency help the interaction of the embedded functions (and eventually trapped molecules) with light. This is especially interesting for applications such as bioreactors, drug delivery, photocatalysis, energy conversion, *etc*.[5] Several silica-based MHTF containing organic functions have been recently synthesised, either by co-condensation[6,7] or post-grafting routes,[8] and a relatively wide choice of functions is beginning to be available. On the other hand, examples of nonsilica functionalised mesoporous materials are scarce, even if methods for the synthesis of transition metal oxide films have been developed, either for MO_2[9] or mixed oxide frameworks,[10] by a general evaporation-induced self-assembly (EISA) procedure.[11] Transition metal (TM) oxide frameworks are interesting for their electronic, mechanical, optical and chemical stability properties. The feasibility of incorporating organic molecules within mesoporous zirconia thin films by post-synthesis grafting was demonstrated by the Sanchez group.[12] However, no efforts to demonstrate a general route to the synthesis and stability of nonsilica-based MHTF were further reported, to the best of the authors' knowledge.

In this work, we report the production of hybrid inorganic-organic mesoporous films based on the post-synthesis functionalisation of cubic titania or zirconia mesostructures with organic bifunctional molecules R–G, which contain a desired R group and a suitable grafting group (G = phosphate, carboxylate, ...) capable of performing complexation of the TM centres. This procedure leads to highly ordered, nonsilica hybrid mesoporous films presenting organic functions at the pore surface. An important aspect of these films is that the anchoring of the organic groups can be varied, from strong and inert (phosphate) to relatively labile (carboxylate), leading to a great flexibility in the attachment of organic functions, which can be advantageously used for different applications (*i.e*., sensors *vs*. controlled release).

Mesoporous MO_2 (M = Ti, Zr) films have been synthesised by dip-coating under controlled conditions, in a similar way as previously described.[12,13] Ethanol–water mixtures containing MCl_4 and triblock copolymer F127 as templating agent were used as precursor solutions (see Experimental). Under the used conditions, highly ordered optical quality cubic *Im*3*m* thin films were synthesised in a two-step procedure (dry atmosphere RH < 20%, followed by exposure to water vapour).[14] The films were stabilised by several post-synthesis treatments in order to optimise the mesostructural resistance to thermal treatment.[15] Stabilised films were thermally treated (300–400 °C) for 1–3 h until complete template removal.

Small angle X-ray scattering using 2D detection (2D-SAXS) patterns and TEM micrographs of stabilised and calcined films (Fig. 1) show that in the reported conditions large pore *Im*3*m* cubic mesostructures with thick amorphous walls are obtained, in agreement with previous work observations. Characteristic vibrational modes of the template (ν_{C-H} at 2850–2920, ν_{C-O-C} at 1038 and 1118 cm^{-1})[16] are absent in FTIR spectra of

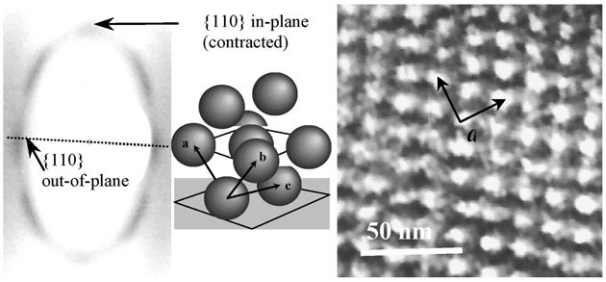

Fig. 1 2D-SAXS (left) and TEM micrograph (along the [100] projection, right) of a ZrO_2 cubic thin film calcined to 350 °C; the dotted line represents the film orientation.

DOI: 10.1039/b415324c

calcined films. Nitrogen adsorption measurements on calcined films (scratched from the substrate) yield Type IV isotherms. For TiO_2, typical surface areas in the range of 150–170 $m^2\ g^{-1}$ and an average pore size of 58 Å[17] were obtained. Film thickness and refraction index were obtained by variable angle ellipsometry. Thickness values are in the 100–300 nm range, depending on the withdrawal speed and sol temperature. As a general rule, thickness grows with increasing withdrawal rate and decreasing sol temperature. From refraction index data, porosity was estimated as 46% of the total volume for TiO_2 and 28% for ZrO_2 (see Experimental); this difference might be attributed to thicker walls in the case of zirconia.

In a subsequent step, mesoporous films were immersed for different time periods into dilute solutions (10^{-2}–10^{-3} M) of the molecules to be grafted. Incorporation of the R functions was followed by FTIR and energy dispersion spectroscopy (EDS), after thorough rinsing of the films to avoid the deposition of organic compound crystals onto the film surface. Incorporation values of carboxylates estimated by EDS are in the 5–8% molecule-to-Ti range, which represents (taking into account a 150 $m^2\ g^{-1}$ surface area[17]), coverage values of 4–7 μmol m^{-2}, in agreement with previously reported values for functionalised mesoporous silica[2] and coverage of TiO_2 surfaces. Maximum uptakes of monododecylphosphate (MDP; no significant changes observed for uptake times $t_{uptake} > 240$ min) are 15% P-to-Ti (12 μmol m^{-2}) throughout the sample. These coverage values are relatively high and might be due to the formation of a bilayer of MDP molecules, favoured by a close interdigitated packing of the aliphatic chains.

FTIR spectra of organically substituted TiO_2 mesoporous films show characteristic bands of organic molecules attached to a titania surface. In contrast, no significant organic amount is found in non-mesoporous films exposed for equivalent times (Fig. 2).

Fig. 2(a) shows the FTIR spectra corresponding to MDP and of substituted mesoporous and non-mesoporous films. Alkyl chain vibrations [ν_{CH} at 2850–2920 cm^{-1}, $\nu_{(CH)n}$ at 1470 cm^{-1}] can be observed, as well as $\nu_{P=O}$, ν_{P-O-R}, ν_{P-O-C} modes overlapped in the 900–1200 cm^{-1} range. The peak pattern in the 900–1000 cm^{-1} region for substituted films (P–O–C and P–OH bands area) is different from the bands observed in pure MDP, suggesting P–OH–Ti interaction.[18] Phenyl vibrations are clearly observed in phenylphosphonate [PPA, Fig. 2(b)] substituted titania [$\nu_{C=C}$ at 1479 cm^{-1}; P=O at 1145 cm^{-1}, C–H out-of-plane (oop) deformation bands between 695 and 755 cm^{-1}]. FTIR spectra of mercaptosuccinic acid [MSA, Fig. 2(c)] show a partial loss of the acid bands ($\nu_{C=O}$ = 1697 cm^{-1}; $\nu_{C=O\ dimer}$ = 1300 cm^{-1}) and the appearance of two bands at 1381 and 1581 cm^{-1} corresponding to the symmetric and asymmetric $\nu_{C=O}$ modes, respectively, is characteristic of bidentate or bridging carboxylate-Ti bonding ($\Delta\nu$ = 200 cm^{-1}).[19] The coexistence of free and bound acid bands suggests that a fraction of the molecules is attached to the titania surface by coordination of one of the carboxylate functions. Similar results are obtained in zirconia-based mesoporous films.

Uptake kinetics experiments performed on MDP incorporated in mesoporous titania (Fig. 3) show that molecule incorporation occurs in two steps and that over 80% of the incorporated MDP enters the pore system within 5 min. The remaining 20% is gradually incorporated and saturation is reached between 60 and 120 min. For thicker films (made by dip-coating at higher deposition speed) the MDP band absorption increases (*i.e.*, more MDP is incorporated, Fig. 3 inset), but in all cases uptake kinetics curves present the same shape and data can be superimposed onto a master curve when normalised to the maximum uptake. EDS also shows that the atomic P-to-Ti ratio is preserved within experimental error, independently of the film thickness. This demonstrates that diffusion across pores of mesoscopic size is not a fundamental

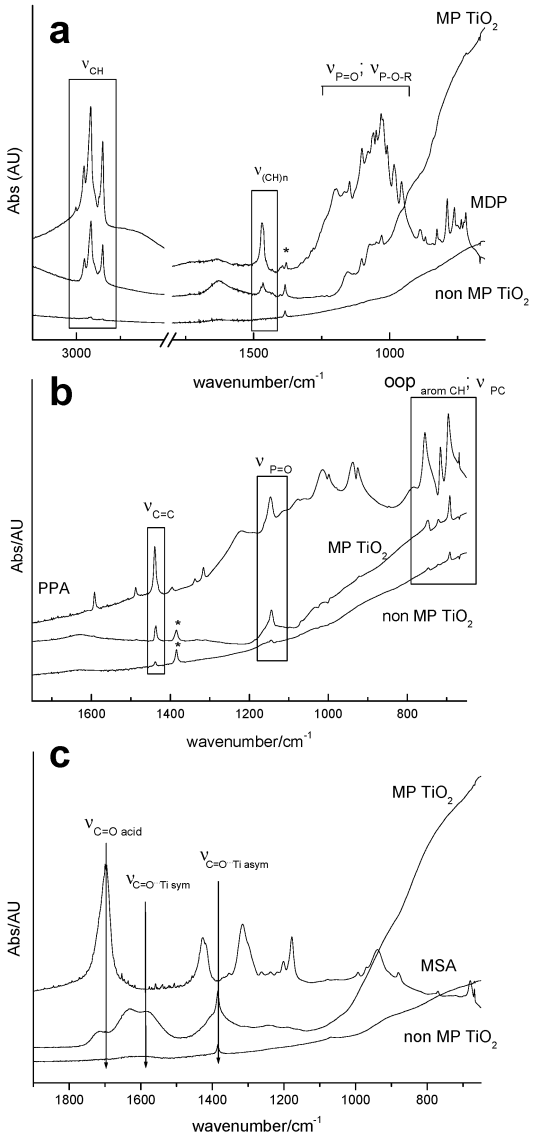

Fig. 2 FTIR spectra of mesoporous titania films exposed to organic molecules: (a) MDP, (b) PPA, (c) MSA. Typical function and skeleton bands are indicated.

limitation in molecule incorporation into thin films presenting a distorted *Im*3*m* cubic mesostructure. MDP uptake depends almost linearly on film thickness (Fig. 3 inset), confirming that MDP molecules can sample the whole film thickness within short times.

To explain the accessibility of pores in these cubic mesostructures, we suppose that the initially unconnected pores stemming from closed micelle mesostructures merge upon thermal treatment, leading to an open pore structure. This has been already proposed for titania films.[20] Similar interconnections between pores have been found in SBA-16 (a caged structure analogous to the ones presented here), in which pore openings develop, depending on the post-synthesis hydrothermal or thermal treatment.[21] Such interconnections are possible thanks to (a) residual wall microporosity, which is favoured in polymer-templated mesostructures, and (b) the formation of necks between pores, related to either to the intrinsic synthesis strategy or to changes in the interpore distance due to changes or shrinkage produced during hydrothermal or thermal treatment.[21] The latter factor is critically dependent on the mesostructure symmetry. Thus, post-synthesis treatment (including the thermal treatment) may play a major role in accessibility when the mesostructure symmetry permits pore fusion. Related results in silica and titania films suggest that the post-synthesis

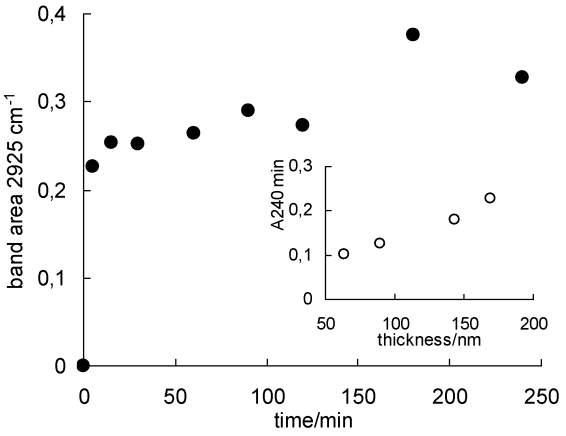

Fig. 3 Variation with time of MDP incorporation in a mesoporous TiO_2 film (measured as the integrated intensity of the ν_{C-H} FTIR band area at 2925 cm^{-1}; film thickness: 2 × 150 nm). Inset: thickness dependence of the saturation absorbance for MDP in mesoporous TiO_2 films (measured as the integrated FTIR absorbance at 240 min, A240).

and thermal treatment steps during template elimination are critical to attain pore accessibility.[22]

Leaching experiments were performed on the functionalised films in order to assess the anchoring of the grafted groups under simulated operating conditions as exchangers, separators or catalysers, as shown in Fig. 4. The complexing groups used for grafting in this work are sensitive to nucleophilic attack by solvent, unlike Si–C_{sp^3} bonds. In the case of MDP/TiO_2 films in THF (t_{uptake} = 2 h), less than 10% of the incorporated function is eliminated within 5 h; this value is unchanged after several days of exposure of the functionalised film to the solvent, suggesting that the remaining MDP is firmly attached to the pore surface. No significant leaching takes place in water, where MDP solubility is lower. Analogous results are obtained with PPA. We conclude that in the case of phosphates or phosphonates, the surface complexation reaction generates a hybrid material with modified pore surface and firmly anchored functions. In the case of carboxylates, higher losses of the original content are generally observed (80–100%). Thioglycolic acid (TGA) is readily lost at pH = 7, suggesting a more labile bond to the TiO_2 surface. A dicarboxylic acid such as MSA is retained for longer times at the same pH, indicating that an extra anchoring group provides a more efficient grafting. MSA leaching rates are higher at lower pH, where the acid is fully protonated,[23] suggesting that carboxylate anchoring groups become more labile at lower pH; the presence of protons probably facilitates the exchange

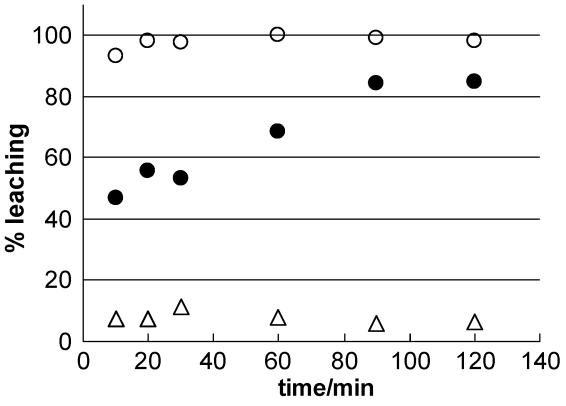

Fig. 4 Leaching of molecules grafted on mesoporous TiO_2 films: (△) MDP in THF, (●) MSA in water, pH = 7.0, (○) TGA in water, pH = 7.0.

of water by the attached carboxylate.[24] This feature can be used in controlled delivery devices, where the release of an anchored drug can be triggered by the external pH.

The trends issuing from leaching experiments demonstrate that the anchoring strength follows the complexation strength of the grafting group, that is, R–O–PO_3^{2-} ~ R–PO_3^{2-} > dicarboxylate > carboxylate, for groups with high solubility in the leaching solvent. An interesting characteristic of these hybrid films is that, contrary to the irreversible grafting observed in mesoporous hybrid silica, anchoring groups with different strengths can be selected to obtain a wide kind of response, from strongly attached functions to functions that can be liberated by external stimuli. Experiments are under way to determine the lability of grafted molecules under varying conditions (*i.e.*, pH change, presence of different nucleophiles, temperature) and after different post-functionalisation procedures, in order to obtain a tailored response. The incorporation of organic molecules in thin films with different mesostructures and thicker particles is addressed separately.[25]

We have demonstrated the possibility to obtain functional mesoporous transition metal oxide (TiO_2 and ZrO_2) thin films, by a post-synthesis method consisting in attaching organic groups to the pore walls. The organic functions are incorporated inside the pore system, as assessed by spectroscopic evidence. All of the *Im3m* film thickness is accessible to the organic function, as diffusion across pores does not seem to limit molecule incorporation. This method could be more generally extended to other M(IV) pure or mixed oxides.

Several key factors control the grafting of functional groups: anchor–M interaction, solubility and solvolytic capability towards the molecule–M complex (modified by pH in the case of exposure to aqueous solutions). A complete set of varied behaviours (from strong grafting to partial leaching to controlled leaching) can be obtained by varying the grafting strength of the group and the leaching solvent. Grafting groups (dicarboxylate, carboxylate, phosphonate, phosphate, ...) present different behaviour towards leaching. While phosphate and phosphonate groups remain strongly attached to the pore walls in solvents with different polarity, carboxylate groups are more labile. This variety of behaviour can be further exploited for a widespread arc of applications, from robust selective sensors to controlled-release smart materials.

Experimental

Materials synthesis

Initial sols were prepared by mixing $TiCl_4$ or $ZrCl_4$ in ethanol with Pluronic F127 [$(EO)_{106}(PO)_{70}(EO)_{106}$] structure directing agent. Chlorides were slowly added under stirring to alcoholic solutions containing the template. Water {h = [H_2O]/[M] = 10 for titania, h = 20 for zirconia} was subsequently added under stirring. The final molar ratio in solution was M : template : H_2O : EtOH = 1 : 0.005 : h : 40. Mesoporous thin films were prepared following a two-step method: dip-coating performed under a dry atmosphere (RH < 20%), followed by a short exposure (10–20 s) to water vapour (adapted from previous work).[12] Clean glass, silicon, polymer (cellulose acetate), KBr pressed pellets or CaF_2 wafers were used as substrates. Film thickness was varied by changing the deposition speed during dip-coating (0.5–4 mm s^{-1}). As-prepared films were submitted to 48 h stabilisation treatments at 50% RH, 60 °C and 135 °C. Thermal treatment of stabilised coatings (up to 350 °C for 3 h) was performed in tubular ovens, under still air, using 1 °C min^{-1} temperature ramps. Further temperature treatment (up to 700 °C) on these films can be performed, leading to a more open pore network.[20] In all cases, non-mesoporous (*i.e.*, dense)

films were produced using the same precursor mixtures in the absence of templates, for control experiments.

Materials functionalisation and function leaching

Monododecyl phosphate (MDP), phenylphosphonic acid (PPA) thioglycolic acid (TGA) and mercaptosuccinic acid (MSA) were used to modify the pore surface by post-grafting. These molecules present different anchoring groups (phosphate, phosphonate, or dicarboxylate). MDP presents a long aliphatic chain and was thus selected for the kinetics experiments in order to optimise the FTIR signal. A typical functionalisation experiment was performed by dipping a calcined mesoporous film, previously rinsed with ethanol and organic-free, in a continuously stirred 0.01 mol dm^{-3} solution of the chosen molecule in a suitable solvent (THF or acetone for MDP and PPA, water for the carboxylic acids). Uptake times (t_{uptake}) were varied from 5 min to several days. After the uptake procedure, the film was rinsed several times with the same solvent and dried in air. Molecule uptake as a function of time was assessed by FTIR and EDS. TiO_2 content in each film was evaluated after film dissolution in hot HCl, by a colourimetric method (TIRON-Ti complex at 380 nm, pH 4.75).

Leaching experiments were performed by introducing a functionalised film with a given t_{uptake} into an appropriate solvent (water at a controlled pH for carboxylic acids, water or THF for MDP and PPA) while stirring. Leaching was evaluated from 5 min to several days by analysing FTIR (KBr or CaF_2 supported films) spectra.

Characterisation

SAXS experiments (transmission or grazing incidence conditions) were performed at the SAXS line in the Laboratório Nacional de Luz Síncrotron, (Campinas, SP, Brazil) using λ = 1.608 Å and a sample-to-detector distance of 650 mm; image plates were used as detectors; thin silicon (8–20 μm) or glass substrates were used. SAXS experiments permitted to completely characterise the samples as cubic *Im3m* mesostructures, in excellent agreement with previous work;[26] uniaxial contraction along z is observed upon thermal treatment. XRD patterns were collected in θ–2θ mode using a conventional goniometer with Cu-Kα_1 radiation. TEM micrographs were collected using a Philips EM 301 transmission microscope (CMA, UBA, Argentina) operated at 65–100 kV. Samples were obtained by scratching the films from the substrate and deposited on Formvar-coated copper or gold grids. Ellipsometry measurements were carried out with a variable angle spectroscopic ellipsometer using porous or dense MO_2 films deposited onto silicon substrates. Optical parameters, that is, thickness (e) and the refractive index (n), were estimated by fitting the obtained ellipsometric ψ and Δ quantities. The refractive index was modelled according to a Maxwell–Garnett effective medium approximation, to take account of pores (inclusions) within a matrix.[27] MP TiO_2 films presented a refraction index n = 1.660, and ZrO_2 films an n = 1.719. The refraction index of the walls (n_{TiO_2} = 2.18 and n_{ZrO_2} = 1.993) was assumed equal to that obtained for nonporous films subject to the same treatment. Thus, the porosity of the ZrO_2 and TiO_2 samples was estimated to be 28 and 46%, respectively.

FTIR spectra were recorded by transmission using a Nicolet Magna 560 instrument. Samples were either observed directly (glass substrate, available region 4500–2000 cm^{-1}), or prepared as KBr pellets. An alternative method consisted in depositing a mesoporous film on a KBr pellet or CaF_2 substrate. All consolidation, thermal treatment and functionalisation steps were performed on these supported thin films, resulting in significant FTIR signal enhancement and a larger IR window. EDS was performed in a Philips SEM microscope equipped with EDAX®.

Acknowledgements

Authors acknowledge funding from CONICET-CNEA (Ph.D. fellowship to PCA), ANPCyT (PICT 06-06631, 06-12345, 06-12057 and 06-10621), UBACyT X093, Fundación Antorchas (RG 14056-18) and Gabbos (Reentry Grant #17-P&G). 2D SAXS measurements were possible thanks to funding from LNLS, Campinas, Brazil (D11A-SAS #2269/03). The authors thank Lic. M. Rosenbusch for her assistance in SEM/EDS and Dr L. Pietrasanta for TEM; Dr P. Morando is kindly acknowledged for his help in FTIR sample conditioning. GJAASI is a CONICET member.

References

1 (*a*) J. L. Shi, Z. L. Hua and L. X. Zhang, *J. Mater. Chem.*, 2004, **14**, 795 and references therein; (*b*) See also: A. Stein, B. J. Melde and R. C. Schroden, *Adv. Mater.*, 2000, **12**, 1403; (*c*) G. Kickelbick, *Angew. Chem., Int. Ed.*, 2004, **43**, 3102; (*d*) T. Asefa, C. Yoshina-Ishii, M. J. Mac Lachlan and G. A. Ozin, *J. Mater. Chem.*, 2000, **10**, 1751.
2 A. Sayari and S. Hammoudi, *Chem. Mater.*, 2001, **13**, 3151.
3 M. H. Lim and A. Stein, *Chem. Mater.*, 1999, **11**, 3285.
4 (*a*) S. R. Hall, C. E. Fowler, B. Lebeau and S. Mann, *Chem. Commun.*, 1999, 201; (*b*) F. de Juan and E. Ruiz-Hitzky, *Adv. Mater.*, 2000, **12**, 430; (*c*) R. J. P. Corriu, A. Mehdi, C. Reyé and C. Thieuleux, *Chem. Commun.*, 2002, 1382; (*d*) W. H. Zhang, X. B. Lu, J. H. Xiu, Z. L. Hua, L. X. Zhang, M. Robertson, J. L. Shi, D. S. Yan and J. D. Holmes, *Adv. Funct. Mater.*, 2004, **14**, 544; (*e*) F. Goettmann, D. Grosso, F. Mercier, F. Mathey and C. Sanchez, *Chem. Commun.*, 2004, 1240.
5 K. Kalyanasundaram and M. Grätzel, *Coord. Chem. Rev.*, 1998, **77**, 347.
6 (*a*) N. Liu, R. A. Assink, B. Smarsly and C. J. Brinker, *Chem. Commun.*, 2003, 1146; (*b*) N. Liu, D. R. Dunphy, P. Atanassov, S. D. Bunge, Z. Chen, G. P. López, T. J. Boyle and C. J. Brinker, *Nano Lett.*, 2004, **4**, 551.
7 (*a*) F. Cagnol, D. Grosso and C. Sanchez, *Chem. Commun.*, 2004, 1742; (*b*) P. Innocenzi, P. Falcaro, S. Schergna, M. Maggini, E. Menna, H. Amenitsch, G. J. A. A. Soler-Illia, D. Grosso and C. Sanchez, *J. Mater. Chem.*, 2004, **14**, 1838.
8 N. Petkov, S. Mintova, B. Jean, T. Metzger and T. Bein, *Mater. Sci. Eng., C*, 2003, **23**, 827.
9 (*a*) G. J. A. A. Soler-Illia, C. Sanchez, B. Lebeau and J. Patarin, *Chem. Rev.*, 2002, **102**, 4093; (*b*) G. J. A. A. Soler-Illia, E. L. Crepaldi, D. Grosso and C. Sanchez, *Curr. Opin. Colloid. Interface Sci.*, 2003, **8**, 109.
10 (*a*) G. J. A. A. Soler-Illia, E. L. Crepaldi, D. Grosso and C. Sanchez, *J. Mater. Chem.*, 2004, **14**, 1879; (*b*) G. J. A. A. Soler-Illia, P. C. Angelomé and P. Bozzano, *Chem. Commun.*, 2004, DOI: 10.1039/B413260B.
11 C. J. Brinker, Y. Lu, A. Sellinger and H. Fan, *Adv. Mater.*, 1999, **11**, 579.
12 E. L. Crepaldi, G. J. A. A. Soler-Illia, D. Grosso, P.-A. Albouy and C. Sanchez, *Chem. Commun.*, 2001, 1582.
13 (*a*) E. L. Crepaldi, G. J. A. A. Soler-Illia, D. Grosso, F. Ribot, F. Cagnol and C. Sanchez, *J. Am. Chem. Soc.*, 2003, **125**, 9770; (*b*) D. Grosso, G. J. A. A. Soler-Illia, F. Babonneau, C. Sanchez, P.-A. Albouy, A. Brunet-Bruneau and A. R. Balkenende, *Adv. Mater.*, 2001, **13**, 1085.
14 E. L. Crepaldi, G. J. A. A. Soler-Illia, A. Bouchara, D. Grosso, D. Durand and C. Sanchez, *Angew. Chem., Int. Ed.*, 2003, **42** 347.
15 E. L. Crepaldi, G. J. A. A. Soler-Illia, D. Grosso and C. Sanchez, *New J. Chem.*, 2003, **27**, 9.
16 G. Socrates, *Infrared and Raman Characteristic Group Frequencies*, John Wiley and Sons, Chichester, 3rd edn., 2001.
17 E. L. Crepaldi, G. J. A. A. Soler-Illia, D. Grosso, F. Cagnol, F. Ribot and C. Sanchez, *J. Am. Chem. Soc*, 2003, **125** 9770.
18 (*a*) G. Guerrero, P. H. Mutin and A. Vioux, *Chem. Mater.*, 2001, **11**, 4367; (*b*) M. I. Tejedor-Tejedor and M. A. Anderson, *Langmuir*, 1990, **6**, 602.
19 G. J. A. A. Soler-Illia, M. K. Boggiano, L. Rozes, C.-O. Turrin, A.-M. Caminade, J.-P. Majoral and C. Sanchez, *Angew. Chem., Int. Ed.*, 2000, **39**, 4249 and references therein.

20 D. Grosso, G. J. A. A. Soler-Illia, E. L. Crepaldi, F. Cagnol, C. Sinturel, A. Bourgeois, A. Brunet-Bruneau, H. Amenitsch, P. A. Albouy and C. Sanchez, *Chem. Mater.*, 2003, **15**, 4562.
21 T.-W. Kim, R. Ryoo, M. Kruk, K. P. Gierszal, M. Jaroniec, S. Kamiya and O. Terasaki, *J. Phys. Chem. B*, 2004, **108**, 11480 and references therein.
22 C. Sanchez, unpublished results.
23 G. E. Cheney, Q. Fernando and H. Freiser, *J. Phys. Chem.*, 1959, **63**, 2055.
24 A. D. Weisz, A. E. Regazzoni and M. A. Blesa, *Solid State Ionics*, 2001, **143**, 125.
25 P. C. Angelomé and G. J. A. A. Soler-Illia, *Chem. Mater.*, in press.
26 G. J. A. A. Soler-Illia, E. L. Crepaldi, D. Grosso, D. Durand and C. Sanchez, *Chem. Commun.*, 2002, 2298.
27 J. C. Maxwell-Garnett, *Philos. Trans. R. Soc. London*, 1904, **203**, 385.